Evaporation Behaviour of a Thinning Liquid Film in a Spin Coating Setup: Comparison Between Calculation and Experiment

José Danglad-Flores[a], Stephan Eickelmann[a], Hans Riegler[a,]

[a] *Max-Planck-Institut für Kolloid- und Grenzflächenforschung, D-14476 Potsdam-Golm, Germany*

Abstract

We present comprehensive measurements of the evaporation behaviour, E, of a thinning liquid film during a hydrodynamic-evaporative spin coating experiment. E, ω (the rotation speed), and ν (the liquid viscosity) are the main control parameters of the process. The evolution of the entire film thinning process can be described theoretically quite well based on the bulk value of ν of the deposited liquid and with a process-specific (constant) E. The weighing in values of ν are easily accessible (calculations, literature values, simple measurements). E is specific for the experimental conditions and values for E cannot be found in literature. There is also no generally accepted strategy to calculate E in advance. We analyzed our experimental results in view of a theoretical prediction for E, which was presented already some time ago by Bornside, Macosco, and Scriven, but never tested experimentally. We find good agreement between theory and experiment for many solvents and different ω. Accordingly, this approach permits *in advance* the calculation of the evolution of the entire hydrodynamic-evaporative film thinning ina spin coating process. In addition, we present a general formula, which allows in the case of spin coating mixtures of volatile solvents and nonvolatile solutes the prediction of the final solute deposit based on literature data only.

Keywords: Evaporation, Spin Coating, Spin Casting, Thin Liquid Films, Final Film Thickness, Final Deposition

1. Introduction

Spin coating is widely used in research and in industrial applications to prepare thin planar films on substrates. In the process, a small amount of liquid is deposited on a rotating planar substrate and spread into a planar film by centrifugal forces. The liquid may be a melt or a solution. Here we will focus on hydrodynamic-evaporative spin casting i.e., spin coating of mixtures of volatile solvents and nonvolatile solutes. After evaporation of the volatile components this process results in the permanent deposition of a thin film of the solute. Typically this solute film is the main purpose of the process. The thickness of the solute film (the solute coverage) can be adjusted through the process parameters. The most relevant parameters are (1) the liquid viscosity, (2) the solute concentration, (3) the rotation speed, and (4) the evaporation behaviour of the liquid.

The thinning of the liquid film and the spatio-temporal evolution of the solute/solvent composition during hydrodynamic-evaporative spin coating have been analyzed in some detail. Meanwhile the process is understood quite well[1–3] and if the physico-chemical process parameters are known,

Email address: hans.riegler@mpikg.mpg.de; telephone:+49 331 567 9236 (Hans Riegler)

in many cases, the final solute coverage can be predicted. In fact, aside from the evaporation rate, all the other relevant spin coating parameters can be obtained rather easily, e.g., from literature or from independent measurements. For instance, the density and viscosity of the solvent/solute mixture can be measured or obtained/calculated from literature data. The rotation speed can be adjusted during the experiment.

Alas, evaporation rates under spin coating conditions cannot be found in literature. They are considered to be rather specific for the experimental conditions (geometry of the spin coating setup, rotation speed, etc.). Therefore, it has been suggested to measure the evaporation rate of a specific solvent for a specific spin coating configuration[2]. This evaporation rate can then be used to calculate the outcome of spin coating processes with the same setup and solvent, but otherwise different process parameters. The relevant evaporation rate can be derived for instance, from the final solute coverage resulting from a "calibration" spin coating experiment. This approach is useful. Nevertheless, it is still desirable to know/calculate the evaporation rate in advance without the necessity of a "calibration" experiment. Thus, one would gain for instance substantial flexibility to pre-select suitable solvents to achieve a desired spin coating result.

Already some time ago, Bornside, Macosco, and Scriven (BMS) proposed how to calculate the evaporation behaviour of volatile liquids in a spin coating configuration [4, 5]. For the calculation only readily accessible literature and process parameter data are necessary. Up to now this theoretical approach has never been tested/confirmed thoroughly by experiment. Presumably this is the case, because 1.) reliable experimental evaporation data were not available and 2.) a concise theoretical description of the spin coating process was not exisiting until recently. Indeed, evaporative film thinning in spin coating configurations has been measured, e.g. by ellipsometry (CITATION). However, until recently it was not clear how meaningful these data were. For instance, it has been discussed whether there exists something like a "simple" evaporation rate at all. It has been questioned whether a single number is meaningful and sufficient to describe in good approximation the evaporative contribution to the film thinning and thus in the end the resulting final solute coverage in the case of solvent/solute mixtures. It was unclear how much the increase of the solute concentration during evaporative film thinning might affect the evaporation rate itself (e.g. via a "skin formation") and thus modify the film thinning process and in particular the resulting final solute deposition. Also, the impact of film dewetting (hole formation) during film thinning (in particular in the late stages of film drying) was not known.

With on-line imaging of the film thinning during the spin coating process it is possible to investigate the film thinning behaviour with high precision[3, 6]. We applied this experimental approach and in the following we will present precise experimental data on the evaporation behaviour derived from the film thinning. The results will be analyzed in in view of the predictions of the BMS approach. We will address in particular whether the BMS theory can be used to quantitatively describe the evaporative contribution to the liquid film thinning in a spin coating process. In addition we will discuss in which cases it is possible to apply this approach for solvent/solute mixtures. Last not least we will show how it can be used to predict the final solute coverage i.e., the main purpose of most spin coating processes.

2. Materials and Methods

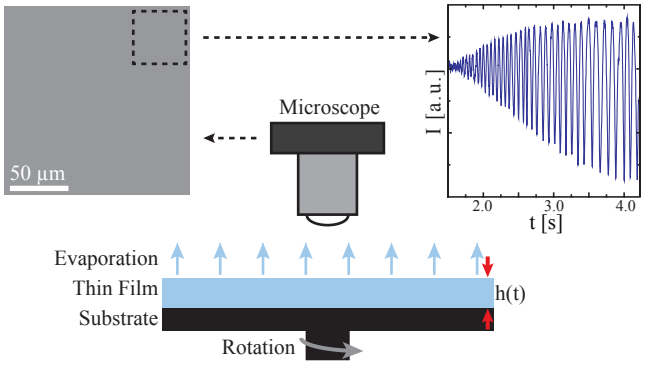

Figure 1: Experimental setup to measure the hydrodynamic-evaporative thinning of a volatile liquid film in a spin coating configuration. The sample surface is imaged via reflection microscopy i.e., with monochrome illumination from the top (through the lens). The interference of the light reflected from the surface of the continuoulsy thinning liquid film and from the interface between the film and the substrate surface modulates the intensity of the reflected light as indicated. The time evolution of the film thickness can be derived from these intensity modulations with great precision. More technical details on the experimental setup (synchronization of the frame rate with the sample rotation, background subtraction, etc.) can be found in [6].

The evaporation rates for various different volatile liquids and liquid mixtures under different spin coating conditions (rotation speeds) were measured with a setup as depicted in Figure 1. In the experiment a drop of the liquid is placed on a solid, planar substrate, which is rotating at a constant speed, ω. After its deposition, the liquid drop rapidly forms a planar film due to centripedal and viscous forces [7]. Due to outward liquid flow and/or spin off at the substrate perimeter, the height, h, of this liquid film is continuously decreasing ($h = h(t)$). With volatile liquids, evaporation also contributes to film thinning. Because viscous shear forces increase rapidly if the film gets thinner evaporative liquid losses increasingly dominate film thinning. For sufficiently thin films the outward liquid flow practically ceases and film thinning only occurs due to evporation. This range of purely evaporative film thinning reveals the evaporation rate, E, with a linear decrease of the film thickness:

$$dh/dt = -E. \tag{1}$$

E can be determined with great precision with the setup depicted in Figure 1 in combination with Equation (1). The range of purely evaporative film thinning can be identified easily, because transition between the (nonlinear) film thinning driven by lateral liquid flow and linear film thinning dominated by evaporation is rather well defined and can be measured experimentally. The transition occurs at (and defines) the so-called transition film height, h_{tr}. h_{tr} is related to E, ν (viscosity) and ω (rotational velocity) according to [1, 8]:

$$h_{tr} = \left(\frac{3E\nu}{2\omega^2}\right)^{1/3}. \tag{2}$$

The transition height, h_{tr}, is *the* key process parameter, because together with the solute concentration it can be used to calculate the final deposit of the solute (see discussion section).

3. Theoretical calculation of E

Some time ago Bornside, Macosko, and Scriven presented a theoretical description of the steady state evaporation behaviour of thin volatile films in a spin coating configuration [4, 5, 9, 10]. They predict an evaporation rate, E, with:

$$E = k\frac{\rho_{vap}}{\rho_{solv}}(x_{solv} - x_{solv,\infty}). \tag{3}$$

Here, ρ_{sol} is the solvent density in its liquid phase and ρ_{vap} is its density in the vapour phase. x_{solv} and $x_{solv,\infty}$ are the solvent mass fractions in the liquid phase and faraway from the liquid in the vapor phase, respectively. k is the mass transfer coefficient.

Assuming Raoult's law to describe the vapour-liquid equilibrium of the solvent and the ideal gas law to estimate its density [4, 5] Eq.(3) can be written as:

$$E = k \left(\frac{P^*_{solv} M_{solv}}{\rho_{solv} R_g T} \right) (x_{solv} - x_{solv,\infty}). \tag{4}$$

P^*_{solv} is the vapour pressure of the pure solvent and M_{solv} is its molecular weight. R_g is the ideal gas constant and T is the temperature.

According to Bornside, Macosco, and Scriven for a planar plate rotating at speed ω the mass transfer coefficient k can be replaced leading to:

$$E = \left(\frac{c D_{solv,air} \omega^{1/2}}{\nu_{air}^{1/2}} \right) \left(\frac{P^*_{solv} M_{solv}}{\rho_{solv} R_g T} \right) (x_{solv} - x_{solv,\infty}). \tag{5}$$

The constant c is a function of the Schmidt number Sc with $c = 0.386 \cdot \mathrm{Sc}^{0.462}$ and $Sc = \nu_{air}/D_{solv,air}$ [11]. $D_{solv,air}$ is the diffusion coefficient of the solvent ($solv$) in air (air) and ν_{air} is the kinematic viscosity of air.

With the approximation $c = 0.386 \cdot \mathrm{Sc}^{0.462} \approx 0.4 \cdot (\nu_{air}/D_{solv,air})^{1/2}$ Eq. (5) can be simplified to:

$$E \approx 0.4 \cdot D^{1/2}_{solv,air} \omega^{1/2} \left(\frac{P^*_{solv} M_{solv}}{\rho_{solv} R_g T} \right) (x_{solv} - x_{solv,\infty}). \tag{6}$$

For pure solvents $x_{solv} = 1$ and $x_{solv,\infty} = 0$, because the solvent concentration in the air far away from the evaporating surface can be neglected. Therefore $(x_{solv} - x_{solv,\infty}) = 1$. Accordingly, Eq. (6) can be simplified further:

$$E \approx \frac{0.4 \cdot D^{1/2}_{solv,air} \omega^{1/2} P^*_{solv} M_{solv}}{\rho_{solv} R_g T}. \tag{7}$$

This is an important result, because all the data necessary to calculate E via Eq. (7) are either available from literature or given by the experimental conditions.

4. Experimental Results

4.1. Evaporation rates for different liquids

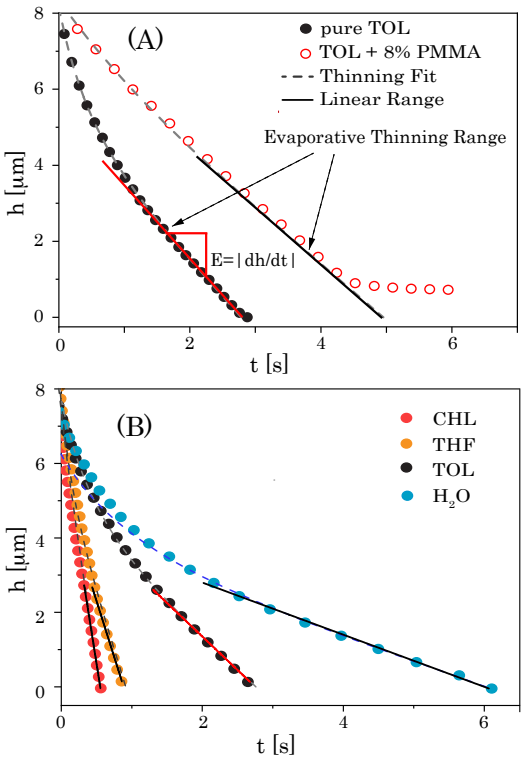

Figure 2: Experimentally measured thinning curves (ω=1000 rpm). The dashed lines are the theoretical fit thinning curves according to the "zero-order" model. The solid lines indicate the linear slope range of the purely evaporative region with $dh/dt = -E$. Panel (A): Pure toluene (TOL) and a solution of toluene with 8% PS-b-PMMA (MW:55k-b-22k). For better visualization the curves are shifted laterally on the time axis. Panel (B): chloroform (CHL), tetrahydrofuran (THF), toluene (TOL), and water (H_2O, 26 °C, relative humidity 40 %).

Fig. 2−A depicts examples of a thinning curve of a pure solvent (toluene) and of a solution of this solvent with 8% PS-b-PMMA (MW:55k-b-22k). For better visualization the curves are shifted laterally on the time axis. The data were measured with the setup depicted in Figure 1. Fig. 2−B presents examples of experimentally observed thinning curves for several pure solvents.

In all cases the region of film thinning dominated by evaporation can easily be identified. It is the range with

the linear decrease in film height, which ends either with the bare substrate (h=0) for the pure solvents or, in the case with the solution containing a nonvolatile component, with a final deposit of film thickness, $h_f = h(t \to \infty)$. The solid lines show the slope of the purely evaporative region with $dh/dt = -E$ according to Eq. (1). The interpretation of the data with respect to the evaporation behaviour is coroborated by the anlysis of the entire thinning curve. The dashed lines are theoretical fits to the experimental date according to the scenario of hydrodynamic-evaporative film thinning as described earlier by the "zero-order" model i.e., neglecting the impact of the solute on the evaporation behaviour [1–3]. This analysis/simulation takes into account both, hydrodynamic and evaporative thinning. The agreement between the experiment and the theory is quite good.

4.2. Evaporation rates for different rotation speeds

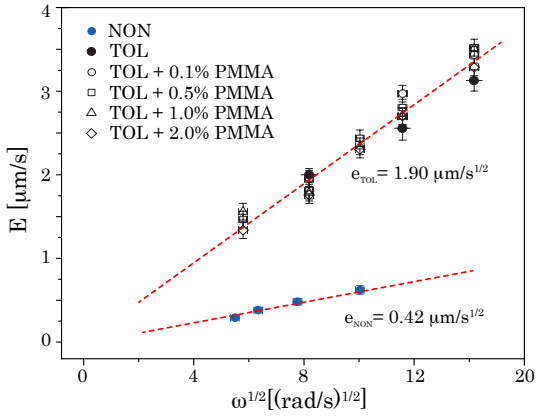

Figure 3: Experimentally measured evaporation rates, E, as function of the square root of the sample rotation, $\omega^{1/2}$. Date are shown for pure n-nonane (NON), pure toluene (TOL), and for various solutions of PS-b-PMMA (MW:55k-b-22k) in toluene (the polymer concentrations are given in mass percentage). The dashed lines show linear fits with slopes indicating the speed-independent evaporation rates e_{TOL} as defined by Eq. (9).

Figure 3 shows evaporation rates, E, as a function of the rotation speed, ω. Data are presented for a pure solvent (nonane) and for solutions of toluene with various concentrations of PMMA. E is plotted as function of the square root of the rotational speed, $\omega^{1/2}$. The dashed lines are fits to the data supporting the validity [1] of Eq. (7) with

$$E \propto \omega^{1/2}. \tag{8}$$

For a better comparison of the data at various rotation speeds it is convenient to rescale the evaporation rates and to define a speed-independent evaporation rate, e, by rewriting Equation (7) accordingly:

$$e = \frac{E}{\omega^{1/2}} \approx \frac{0.4}{R_g T}\left(\frac{D_{solv,air}^{1/2} P_{solv}^{*} M_{solv}}{\rho_{solv}}\right). \tag{9}$$

.

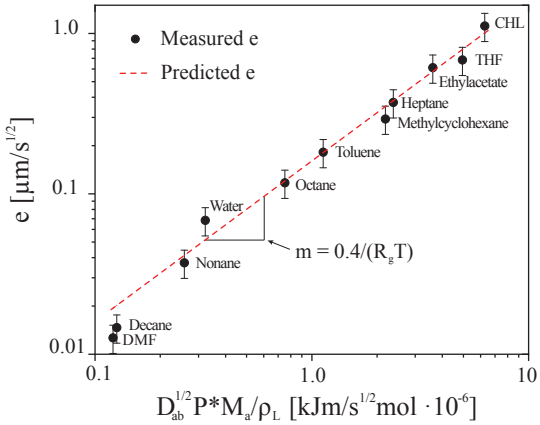

Figure 4: Experimentally measured speed-independent evaporation rates, e, for various solvents as function of the pure solvent properties ($D_{ab}P^{*}M_a/\rho_L$). The dashed line shows a linear fit (Pearson coefficient = 0.996) through the origin. Its slope is 1.6×10^{-4} mol/J.

Figure 4 presents evaporation data for many different pure solvents and mixtures of solvents with nonvolatile solutes (with relatively low solute concentrations). The data are plotted according to Eq. (9) with the physico-chemical data for the different systems obtained from literature (see appendix). Motivated by Eq. (9) the dashed straight line in Figure 4 has a slope of $0.4/(R_g T)$ with $T = 26°C$, the

[1] For simplicity it is assumed for the fits that that $E(\omega = 0) = 0$), because the experimental data are not accurate enough to conclude/predict by extrapolation ($E(\omega \to 0)$) with sufficient significance the (small) evaporation rates for $\omega = 0$.

experimentally applied temperature.

5. Discussion

5.1. General remarks

Evaporation rates in a spin coating configuration, $E(\omega)$, were measured for different rotation speeds, different solvents, and various solvent/solute mixtures by direct observation of the film thinning. The measurements via on-line imaging show that the evaporating liquids form closed and planar films throughout the entire film thinning process. Thus it is assured that the evaporative film thinning agrees with the scenario assumed for a typical spin coating process as it is described by the corresponding theory.

It is observed that the evaporation rates are proportional to $\omega^{1/2}$. This behaviour and the absolute numbers measured for E are in good quantitative agreement with a theoretical prediction published some time ago by Bornside, Macosko, and Scriven [4, 5]. This means that E can directly be calculated from literature data of the solvent properties and from readily available process parameters. More so, it means that it is possible to quantitively calculate *in advance* the entire film thinning process during the spin coating process including its result, the deposition of the solute.

5.2. Validity and limitations of the approach

Quite remarkable, the technical specifications of the spin coating setup, such as for instance the size/diameter of the substrate, are not taken into account by the BMS approach. It is rather unlikely that the technical conditions of our setup just by chance lead to the quantitative agreement between theory and experiment. It can be assumed, that under spin coating conditions, which are roughly similar our case i.e., with substrate dimensions of a few *cm* in diameter, and with a similar experimental protocol (e.g., deposition of an excess volume on the already rotation sample), the evaporation rates can be calculated quite accurately via the BMS approach.

It has to be considered that the approach presented in this report will be of limitied applicability for 1.) non-Newtonian liquids, 2.) if the liquids do not wet completely the substrate, or 3.) if the liquid viscosity is very sensitive to temperature (because during film film thinning there is evaporative cooling). Also, with liquid mixtures of two or more volatile components the evaporation behaviour and thus the film thinning behaviour may not be described correctly by assuming a (constant) evaproation rate calculated with (the approach leading to) Eq. (7). Even if the calculation of E with an appropriately modified (for mixtures) Eq. (7) yields a correct evaporation rate for thick planar films, Marangoni effects may influence the thinning behaviour of thin films. This may cause surface undulations the late stages of film thinning and thus, for instance to film rupture. Last not least, miscibility gaps may affect E and ν.

With solutions of volatile solvents and nonvolatile solutes another aspect has to be considered. In this case the film thinning process can be described quantitatively by takiing int account the true solution viscosity. [2, 3]. This means, that the weighing in viscosity of the *solution* (and not that of the *solvent*) has to be taken into account to calculate the film thinning behaviour, because even with small solute concentrations, the viscosity of the solution can be very different to the viscosity of the pure solvent. With the weighing in solution viscosity, ν, an evaporation rate, E, calculated with Eq. (7) for the pure solvent, the applied ω, the film thinning behaviour can be calculated/predicted quite accurately (except for the late stages

with high solute concentration) E calculated via Eq. (7) assuming pure solvent properties can be taken in this case for the calculations, because the evaporation rates of pure solvent and solution are quite similar as long as the solute concentrations does not exceed 10-20% due to evaporative enrichment. In the very late stages of film thinning the deviation between experiment and calculation is very significant, because solute deposition is not explicitly take into account in the zero order approach. Nevertheless, because the amount of solute deposition is determined by the early stages of the hydrodynamic-evaporative film thinning, taking into account the true weighing in solute viscosity is sufficient to quite accurately predict the amount of final solute.

5.3. Estimation of the solute deposition

The final solute film thickness can be calculated with the spin coating parameters via the transition height, h_{tr} (see Eq.(2)) as follows [1–3]:

$$h_f \approx x_0 \cdot h_{tr}. \tag{10}$$

This equation assumes identical densities of the solvent and the solute and x_0 denotes the volume ratio between solute and solvent in the initial (weighing in) solution.

With different densities of solvent, ρ_{solv}, and solute, ρ_{solu}, Eq. (10) has to be modified:

$$h_f \approx x_0 \cdot \frac{\rho_{solv}}{\rho_{solu}} \cdot h_{tr}. \tag{11}$$

If the solute concentration is given as c_0 i.e., as an entity per volume (e.g., moles or particles per volume), deposition leads to a final coverage of the solute in entity per area, Γ_0:

$$\Gamma_f \approx c_0 \cdot \frac{\rho_{solv}}{\rho_{solu}} \cdot h_{tr}. \tag{12}$$

It should be noted that ρ_{solu} denotes the *average* density of the solute. This is important, for instance, in the case of metal nanoparticles coated with a shell of organic molecules. In this case ρ_{solu} results from the weight of the particle core plus its shell divided by the volume of the entire particle (core and shell).

5.4. The final "master" equation

The combination of Eq.(11) or Eq.(12) with Eq.(7) yields a general "master" formula to predict the final film thickness:

$$h_f \approx 0.85 \cdot x_0 \cdot \frac{\rho_{solv}}{\rho_{solu}} \cdot \left[\frac{\nu D_{solv,air}^{1/2} P_{solv}^{*} M_{solv}}{\omega^{3/2} \rho_{solv} R_g T} \right]^{1/3}. \tag{13}$$

or the final coverage:

$$\Gamma_f \approx 0.85 \cdot c_0 \cdot \frac{\rho_{solv}}{\rho_{solu}} \cdot \left[\frac{\nu D_{solv,air}^{1/2} P_{solv}^{*} M_{solv}}{\omega^{3/2} \rho_{solv} R_g T} \right]^{1/3}. \tag{14}$$

The assumptions leading to Eqs.(11) and (12) indicate an accuracy of about ±10%. Assuming similar margins for Eq.(7) based on the experimental results presented in Fig. 4, suggests an accuracy of typically ±(20)% or better for the final master Eqs.(13) and (14). This is consistent with the experimental data of Figs.3 and 4.

6. Summary and Conclusion

We have measured the evaporation rates, E, of many different volatile solvents and mixtures of volatile solvents and non-volatile solutes during a hydrodynamic-evaporative spin coating process. This process describes the evolution

of a planar, continuously thinning liquid film on a rotating substrate. Recently it has been analyzed theoretically in some detail. The film thinning during the spin coating process is essentially determined by three control parameters: 1.) the evaporation rate, E, 2.) the liquid viscosity, ν, and 3.) the rotation speed, ω. With solutions of a volatile solvent and a nonvolatile solute, a final deposit of the solute remains after complete evporation of the solvent. The amount of final deposit can be calculated from the solute concentration, x_0, of the solution at the beginning of the process. Three of these parameters, ω, ν , and x_0, are readily available prior to the spin coating process. They can either be adjusted, easily measured, obtained from literature, or calculated from literature data. Data on E, on the other hand, are not readily available from literature for several reasons. E is considered to be specific for the experimental setup. It is also rather hard to measure E under spin cast conditions. Last not least, there is no generally accepted way how to calculate E, because it may change during the process. Yet, already some time ago Bornside, Macosco, and Scriven presented a way to calculate E from literature data. Up to now, their proposal has never beeen tested by experiment. We present experimental data for E and we analyze them in view of their proposal. We find that their theoretical calculation of E agrees remarkably well with our experimentally measured E for many different solvents and spin cast conditions. We combined their approach with the recent quantitative theoretical analysis of spin coating. Because E can be calculated from literature data the entire spin coating process can be calculated in advance. This is in particular important in the case of solutions containing nonvolatile solutes, which will be deposited in the course of the process. Quite often the controlled deposition of the solute is the main purpose of the spin cast process. We present a formula to calculate in advance the final solute coverage solely based on readily available (literature) data. Thus the desired solute coverage can be adjusted in advance through the selection of the solvent and/or the rotation speed.

Acknowledgements—Thanks to Reinhard Lipowsky for institutional support. JDF was funded by the DAAD and DFG through the IRTG 1524. JDF thanks for his training the GISDE, Universidad de Oriente, Venezuela.

Conflict of Interest—Authors have no conflict of interest relevant to this article.

[1] S. Karpitschka, C. M. Weber, H. Riegler, Spin casting of dilute solutions: Vertical composition profile during hydrodynamic-evaporative film thinning, Chemical Engineering Science 129 (2015) 243–248.

[2] J. Danglad-Flores, S. Eickelmann, H. Riegler, Deposition of polymer films by spin casting: A quantitative analysis, Chemical Engineering Science 179 (2018) 257 – 264.

[3] J. Danglad-Flores, K. Eftekhari, A. G. Skirtach, H. Riegler, Controlled deposition of nanosize and microsize particles by spin-casting, Langmuir 35 (9) (2019) 3404 – 3412.

[4] D. Bornside, C. Macosko, L. Scriven, Spin coating of a pmma/chlorobenzene solution, Journal of the Electrochemical Society 138 (1) (1991) 317–320.

[5] D. E. Bornside, R. A. Brown, P. W. Ackmann, J. R. Frank, A. A. Tryba, F. T. Geyling, The effects of gas phase convection on mass transfer in spin coating, Journal of Applied Physics 73 (2) (1993) 585–600.

[6] S. Eickelmann, H. Riegler, Rupture of ultrathin solution films on planar solid substrates induced by solute crystallization, Journal of colloid and interface science 528 (2018) 63–69.

[7] A. G. Emslie, F. T. Bonner, L. G. Peck, Flow of a viscous liquid on a rotating disk, Journal of Applied Physics 29 (5) (1958) 858–862.

[8] O. S. Cregan V, A note on spin-coating with small evaporation, Journal of Colloid and Interface Science 314 (2007) 324–328.

[9] Y. Chang, W. Wu, W. Chen, Theoretical analysis on spin coating of polyimide precursor solutions, Journal of The Electrochemical Society 148 (4) (2001) F77–F81.

[10] J. J. van Franeker, D. Westhoff, M. Turbiez, M. M. Wienk,

V. Schmidt, R. A. Janssen, Controlling the dominant length scale of liquid–liquid phase separation in spin-coated organic semiconductor films, Advanced Functional Materials 25 (6) (2015) 855–863.

[11] F. Keith, J. Taylor, J. Chong, Heat and mass transfer from a rotating disk, Tech. rep., DTIC Document (1958).

[12] I. Smallwood, Handbook of organic solvent properties, Butterworth-Heinemann, 2012.

[13] R. M. Felder, R. W. Rousseau, L. G. Bullard, Elementary Principles of Chemical Processes, Wiley Global Education, 2015.

[14] T. R. Marrero, E. A. Mason, Gaseous diffusion coefficients, Journal of Physical and Chemical Reference Data 1 (1) (1972) 3–118.

[15] H. Y. Erbil, Y. Avci, Simultaneous determination of toluene diffusion coefficient in air from thin tube evaporation and sessile drop evaporation on a solid surface, Langmuir 18 (13) (2002) 5113–5119.

[16] G. Lugg, Diffusion coefficients of some organic and other vapors in air, Analytical Chemistry 40 (7) (1968) 1072–1077.

[17] W. J. Lyman, W. F. Reehl, D. H. Rosenblatt, Handbook of chemical property estimation methods: environmental behavior of organic compounds, Washington, DC (United States); American Chemical Society, 1990.

[18] J. Coca, J. Bueno, R. Alvarez, Gaseous diffusion coefficients by the stefan-winkelmann method using a polymer-solvent mixture as evaporation source, Ind. Eng. Chem. Fundam. 19 (2) (1980) 219–221.

[19] A. Berezhnoi, A. Semenov, Binary Diffusion Coefficients of Liquid Vapors in Gases, Begell House, 1997.

7. Appendix

Physico-chemical properties of the solvents

Table 1: **Physico-chemical properties of the solvents at 298,15K**. The unmarked data for density (ρ_{solv}), molecular weight (M_{solv}), kinetic viscosity (ν_{solv}), and vapor pressure P^*_{solv} (estimation by the Antoine equation) are from Ref. [12]. The data marked by * are from Ref. [13]. The data for the diffusion coefficients in air ($D_{solv,air}$) are from: ** Ref.[14], ‡ Ref.[15], † Ref.[16], ! Ref.[17], § Ref. [18], $ Ref.[19].

Solvent	$\rho_{solv}[kg/m^3]$	$M_{solv}[10^{-3}kg/mol]$	$P^*_{solv}[10^3Pa]$	$D_{solv,air}[10^{-6}m^2/s]$	$\nu_{solv}[10^{-7}m^2/s]$
Water	1000	18	3.37	25.1**	8.93
Toluene	867	92	3.79	8.03‡	6.34
Ethyl acetate	902	88	12.6	8.61†	4.72
Chloroform	1483	119	26.2	8.88†	3.65
Tetrahydrofuran	889	72	21.6	11.1§	5.17
Dimethylformamide	944	73	0.502	9.73†	8.5
n-Heptane	684	100	6.11	7.05!	5.5
n-Octane	703	114	1.86	6.16†	7.25
n-Nonane	718	128	0.572	6.43!	8.65
n-Decane	730	174	0.22	5.74!	11.8
Methylcyclohexane	770	98	6.05*	6.15$	8.7

Speed-independent evaporation rates of the solvents

Table 2: **Speed-independent evaporation rates: Experimental results (e) and calculated numbers ($\mathbf{e_{th}}$)**. The measured evaporation rates, e, are also presented in Fig. 4 of the main text. The theoretical evaporation rates, e_{th}, are calculated using Eq.(8) (see below and main text) with the physico-chemical properties given by Table 1 and with $R_g = 8.31\,\mathrm{J\,mol^{-1}\,K^{-1}}$, $\omega = 16.7\,\mathrm{s^{-1}}$ (=1000 rpm), $T = 299.15\,\mathrm{K}$ (= 26 °C), $RH_{H_2o} = (40 \pm 1)\%$.

Solvent	$e[10^{-6}m/s^{1/2}]$	$e_{th}[10^{-6}m/s^{1/2}]$
Water	0.07	0.05
Toluene	0.18	0.19
Ethyl acetate	0.61	0.58
Chloroform	1.11	1.01
Tetrahydrofuran	0.68	0.80
Dimethylformamide	0.01	0.02
n-Heptane	0.37	0.39
n-Octane	0.12	0.12
n-Nonane	0.04	0.04
n-Decane	0.01	0.02
Methylcyclohexane	0.29	0.35